7th EDF & LMS Poitiers Workshop: "Operational Limits of Bearings:
Improving of Performance through Modelling and Experimentation"

Futuroscope, October 2, 2008

Low frequency shaft vibration tests and analyses
Analyses et essais sur les vibrations basse fréquence de l'arbre en rotation.

DeCamillo S[a], Cloud CH[b], Byrne JM[b] and He M[b]

[a] Kingsbury, Inc., 10385 Drummond Road Philadelphia, PA 19154, USA.

[b] BRG Machinery Consulting, LLC, 703 Highland Avenue, Charlottesville, Virginia 22903, USA.

Tilt pad journal bearings are well known for overcoming vibration limitations of fixed geometry bearings. There are, however, other vibration phenomena associated with tilt pad bearings that are topics of past and present research. Over the past few years, unusual, low-frequency, radial vibrations have been observed in different types of machines using tilt pad journal bearings. The vibrations are not like sharp, subsynchronous spikes that often indicate a serious problem. They are of low frequency and amplitude, and fluctuate randomly. These low level vibrations have raised concern in acceptance tests of critical machinery, even in cases that comply with industry specifications, because their cause and nature are unknown.

This paper presents shaft and pad vibration data from tilt pad journal bearing tests that were performed to investigate and better understand these subsynchronous indications. The low frequency vibrations are compared under the influence of speed, load, oil flow, and bearing orientation. Results are presented for conventional and direct lube tilt pad bearings, along with discussions of parameters and methods that were successful in reducing and eliminating these low level vibrations.

Theoretical analyses are also presented and discussed in relation to the test observations. The analyses use an algorithm that accounts for effects when there is insufficient flow for the oil films, and the resulting full matrix dynamic coefficients are used to examine the frequency response characteristics of each pad in relation to test measured pad vibration. The model correlates well with test results, thereby providing a useful tool to assess the effects of multiple factors and complex pad/shaft interactions that influence these low level vibrations.

The intention is that this information will be of value to researchers, analysts, and other personnel involved with design and prediction of hydrodynamic bearings in high-speed machinery.

Les paliers à patins oscillants sont connus pour surmonter les limitations imposes par les vibrations qui existent pour les paliers à géométrie fixe. Il existe cependant d'autres phénomènes vibratoires sur les paliers à patins oscillants qui sont l'objet de recherches passées et présentes. Depuis quelques années, des vibrations radiales, inhabituelles, de fréquence basse, ont été observées sur différents types de machines comportant des paliers à patins oscillants. Ces vibrations ne sont pas des pics transitoires sous synchrones qui indiquent souvent un problème grave. Elles ont une fréquence basse et une faible amplitude, et fluctuent aléatoirement. Ces vibrations de bas niveau ont soulevé l'inquiétude dans des contrôles de réception des machines critiques, même dans les cas qui sont conformes aux caractéristiques d'industrie, du fait de leur cause et de leur nature inconnues.

Afin de mieux comprendre ce phénomène de vibration sous synchrone, cette étude présente les données de vibration de l'arbre et d'un patin issus de tests qui ont été réalisés sur un palier à patins oscillants. Les vibrations de basse fréquence sont comparées en faisant varier la vitesse, la charge, le débit et de l'orientation du palier. Les résultats sont présentés pour des paliers avec une alimentation conventionnelle ou directe, et discutés en fonction des paramètres et des méthodes mises en œuvre pour limiter et éliminer ces vibrations de basse fréquence.

Les analyses théoriques sont également présentées et discutées par rapport aux résultats expérimentaux. Elles sont réalisées grâce à un algorithme qui prend en compte les effets d'une sous alimentation, et la matrice complète des coefficients dynamiques en résultant est employée pour examiner les caractéristiques de réponse en fréquence de chaque patin par rapport à la vibration mesurée lors des essais. La corrélation entre le modèle et les résultats expérimentaux est satisfaisante, fournissant de ce fait un outil utile pour évaluer les effets des facteurs multiples et des interactions complexes de patin/arbre qui influencent ces vibrations.

Keywords : hydrodynamic, tilt pad journal bearing, subsynchronous vibration
Mots-clés : hydrodynamique, palier à patins oscillants, vibration sous-synchrone.

1. SSV Hash

Figure 1 is an example radial vibration spectrum from a high-speed compressor using tilt pad journal bearings. The subject of this paper is the low-frequency shaft vibrations indicated in the figure. The term *SSV hash* is defined for use in this paper to distinguish the subsynchronous vibration (SSV) characteristics under consideration:

SSV Hash: A vibration signature characterized by low-frequency, low amplitude, broadband subsynchronous vibrations that fluctuate randomly.

Field experience of SSV hash has been for smaller journal bearings, approximately 100 to 200 mm in diameter. When it occurs, SSV hash typically ranges up to 30 Hz with amplitudes on the order of .0025 to .0050 mm peak-to-peak. The signature has been encountered in turbines, compressors, and gear boxes using conventional bearings, which have seals to flood the bearing cavity, as well as direct lube bearings that are typically designed for an evacuated configuration.
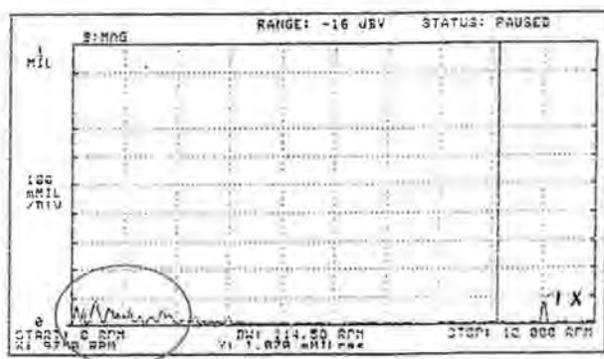

Figure 1. Example low-frequency, broadband, vibration.

2. Experimental Studies

Uncertainty regarding the nature and significance of SSV hash prompted a series of tests performed on Kingsbury's high-speed rig (Figure 2), which has a test shaft driven by a gas turbine through a flexible coupling. The shaft is 1.5 meters long and 127 mm in diameter, supported at either end by pivoted shoe journal bearings. Proximity probes are mounted inboard of each journal to record shaft vibration.

It was possible to duplicate the compressor signature on the test rig. Results from initial tests in 1999/2000 are reported in reference [1], summarized here for convenience: Direct lube bearings were investigated at 10,000 rpm and 0.14 MPa projected load. In the as-designed evacuated configuration, increasing flow tended to reduce amplitudes but did not entirely eliminate SSV hash. Elimination required installation of floating oil seals and an increase in oil flow, resulting in higher power loss, pad temperatures, and oil flow than the original design. A modification was conceived where *SSV grooves* were cut in the babbitt face to capture and redirect side leakage towards the leading edge of the next pad [2], which was successful in eliminating SSV hash in the evacuated configuration. Low oil flow and power loss of the original design were maintained, with a slight penalty in pad temperature due to the introduction of warm, side leakage oil back into the oil film.

7th EDF & LMS Poitiers Workshop: "Operational Limits of Bearings:
Improving of Performance through Modelling and Experimentation"

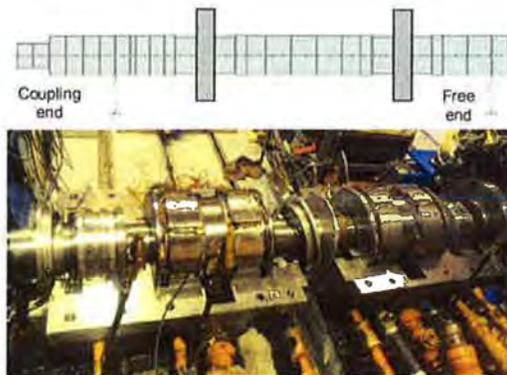*Futuroscope, October 2, 2008*

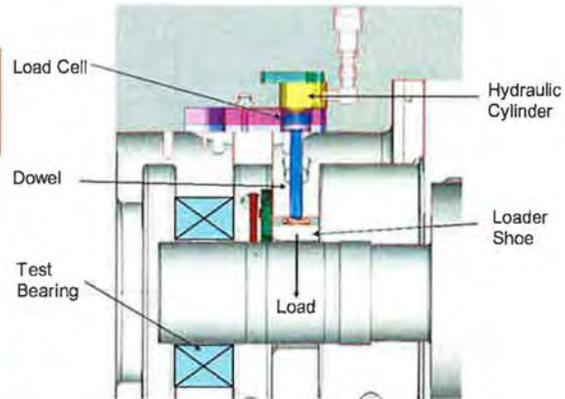Figure 2. Test rig journal bearings and shaft schematic.

Figure 3. Radial load system schematic, free end of shaft.

2.1 Subsequent tests.

While two solutions were obtained in initial tests, conditions were limited. The rig was modified with a load system at the free end of the shaft for subsequent tests (Figure 3). A hydraulic cylinder loads a single loader shoe that pushes down on the shaft and loads the test bearing. A load cell measures applied load.

The test bearings (Figure 4) consist of a conventional center pivot bearing with labyrinth end seals and evacuated direct lube center and offset pivot bearings. Three direct lube methods were tested: spray nozzles, leading-edge-grooves (LEG®) and between-pad-grooves (BPG®). Bearings were 127 mm diameter by 57 mm long with steel backed babbitted pads, 60 degree angle, 0.18 mm diametric clearance, and 0.25 nominal preload. Tests were run with ISO VG 32 oil supplied at 49 °C.

Figure 4. Test bearings: a) conventional with laby seals, b) spray nozzle, c) LEG®, d) BPG®.

Loads in following figures refer to the applied load. For data labeled no-load, the bearings support the shaft weight (0.14 MPa projected load). Test bearings were installed around the free end of the shaft. The coupling end journal bearing was not changed. Vibration data were recorded while varying speed to 14,000 rpm, load to 2.8 MPa, and oil flow to 114 l/min, holding two of the parameters constant while the other was varied. Each bearing was tested for load-on-pad (LOP) and load-between-pad (LBP) orientation.

Only the speed ramp data are used in this paper for reference, presented in color-coded FFT waterfall diagrams. With Figure 5 as an example, each diagram contains three separate run-up/run-down speed ramps from 5,000 to 14,000 to 5,000 rpm (83 to 233 to 83 Hz), one for each of three oil flows. Vertical scale denotes peak-to-peak amplitude in mils, one mil equals .0254 mm. The back plane of the diagram contains a projection of all data. The data are uncompensated, the main focus being the low-frequency vibrations.

2.2 Shaft SSV hash trends

The volume of data for different bearing designs allowed an assessment of shaft SSV hash trends. Conventional bearing speed ramp data in Figures 5 through 8 are used for examples.
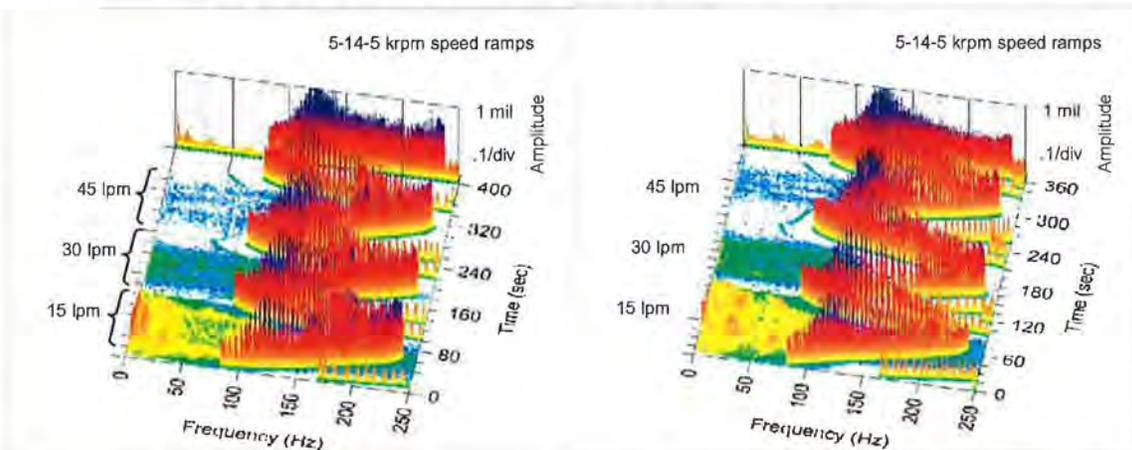

Figure 5. Conventional center pivot, LBP, no-load.

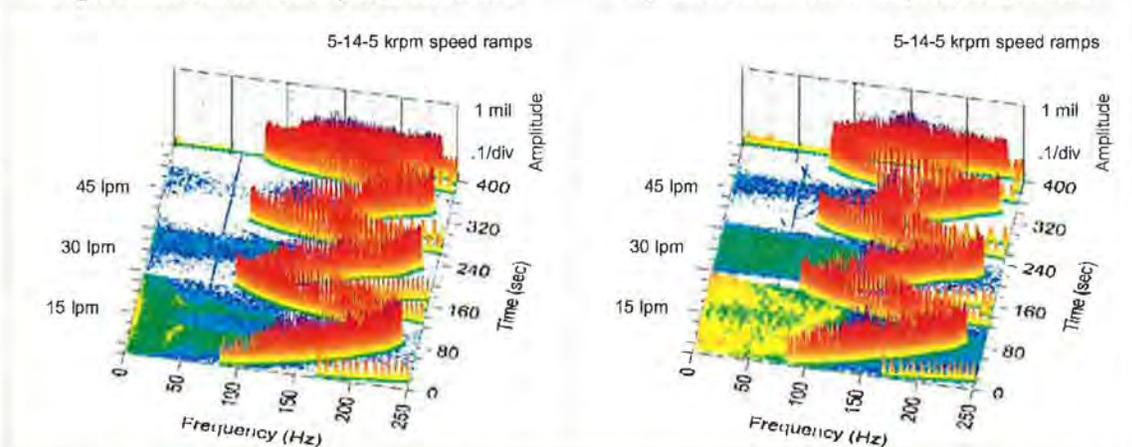Figure 6. Conventional center pivot, LOP, no-load.

Figure 7. Conventional center pivot, LBP, 2.8 MPa.

Figure 8. Conventional center pivot, LOP, 2.8 MPa.

The following trends were found to be fairly common among all bearing designs: Viewing the figures, it can be noticed that most SSV hash indications occur at low flow and low load. SSV hash levels for no-load data were similar for LBP and LOP orientations (e.g. Figure 5 vs. 6), and decreased with applied load for LBP orientation (e.g., Figure 5 vs. 7) where there was less of a reduction for LOP orientation (e.g., Figure 6 vs.8).

It is worth noting that initial reports and tests were for high-speed applications with light rotors, so SSV hash was formerly associated with high-speed and low-load. The data in these subsequent tests indicate that this is not exactly true. There can be undesirable levels in the case of load-on-pad orientation at higher loads, for example Figure 8 at 2.8 MPa. There were also many indications at lower speeds, as can be seen in Figures 5, 6 and 8.

7th EDF & LMS Poitiers Workshop: "Operational Limits of Bearings:
Improving of Performance through Modelling and Experimentation"

Futuroscope, October 2, 2008

2.3 Conventional vs. direct lubrication

Figure 9 is conventional bearing data, flooded configuration, from Figure 6 zoomed in on the lower frequencies and amplitudes under investigation. Figure 10 is comparable between-pad-groove direct lube data, evacuated configuration. Comparisons are straight forward. Direct lube data has noticeable SSV hash indications at 30 l/min whereas conventional bearing levels are negligible. Conversely, very high subsynchronous vibrations are noticeable in conventional bearing data at 15 l/min where the direct lube design has significantly lower SSV hash indications.
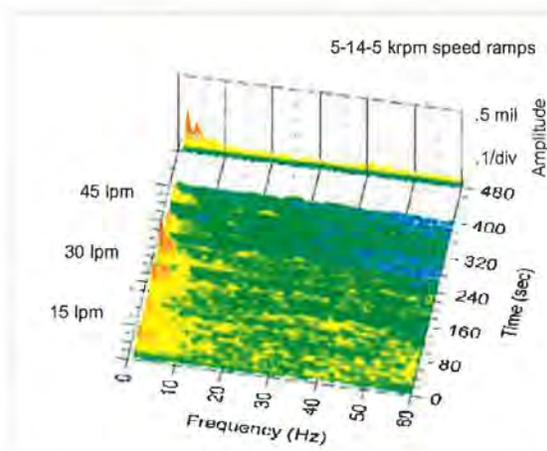

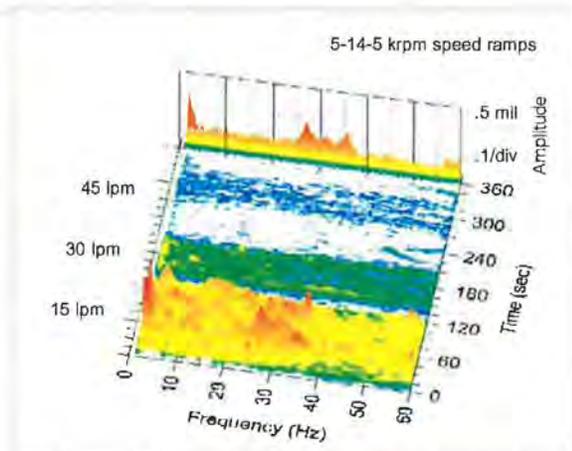Figure 10. Direct lube BPG, center pivot, LOP, no-load.   Figure 9. Conventional center pivot, LOP, no-load.

The direct lube data follow general trends in that there are more SSV hash indications at low flow. The word *indication* is carefully used in the generalization because higher *amplitudes* sometime occur at other conditions, e.g. 30 l/min in the case of Figure 10. Figure 10 also supports observations in initial investigations [1] where SSV hash decreases, but is not necessarily eliminated at higher flows.

2.4 Variations among direct lube designs

Three offset pivot direct lube bearings were tested to compare their effect on SSV hash; spray nozzles, LEG, and BPG (reference photographs in Figure 4). All have an evacuated discharge configuration. In general, all three direct lube designs display noticeable SSV hash (Figure 11). Variations in amplitudes and frequencies make it difficult to generalize results. The spray nozzle design produced the highest levels of SSV hash. The LEG operated with lower SSV hash amplitudes but at higher frequencies, and BPG SSV hash levels were lower for most conditions in comparison with spray nozzle data. BPG vs. LEG results vary. SSV hash levels at 15 l/min are negligible and lower than the LEG. At higher flows, BPG SSV hash amplitudes are higher but occur at a lower frequency.
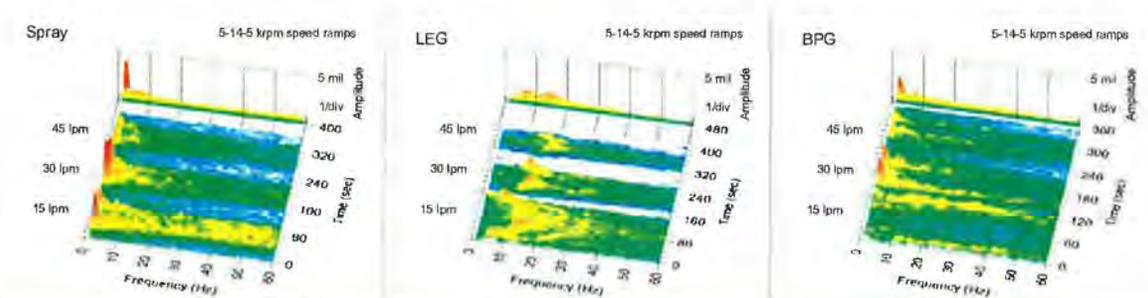

Figure 11. Direct lube comparisons, LOP, no-load.

Distinct differences in shaft SSV hash signatures are obvious among the designs. Some speed dependence is noticeable in spray nozzle data, and more so in LEG data. BPG characteristics do not show variations with speed, and seem sensitive only at a particular speed depending on flow.

2.5 Pad/Shaft Correlation

An upper and a lower pad were monitored with proximity probes in prior tests to investigate pad vibration as a possible source of shaft SSV hash. Unfortunately, an unexpected result was that there were few correlations with shaft SSV hash for the broad range of conditions and bearings tested. The lack of correlation prompted another series of tests with all pads monitored by proximity probes, which are mounted in the casing, targeting the trailing edge of the back of the pads at locations as depicted in Figure 12.
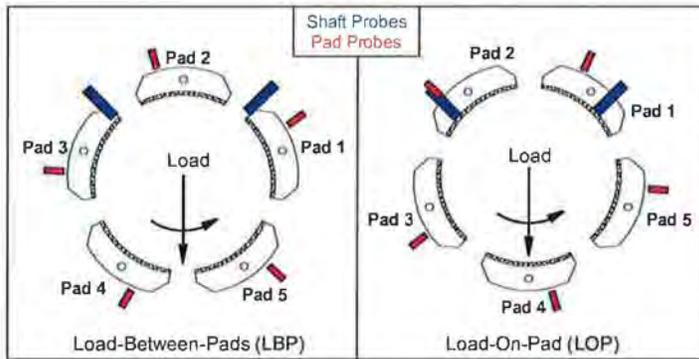

Figure 12. Bearing Orientation and Pad Numbering.

Figure 13 organizes shaft and pad data for a leading-edge-groove bearing test at 1.38 MPa for a load-on-pad configuration. The waterfall diagrams are arranged so that data for the shaft probes and all five pads can be viewed in relation to one another. The same scales are used for all waterfall diagrams in the figure.
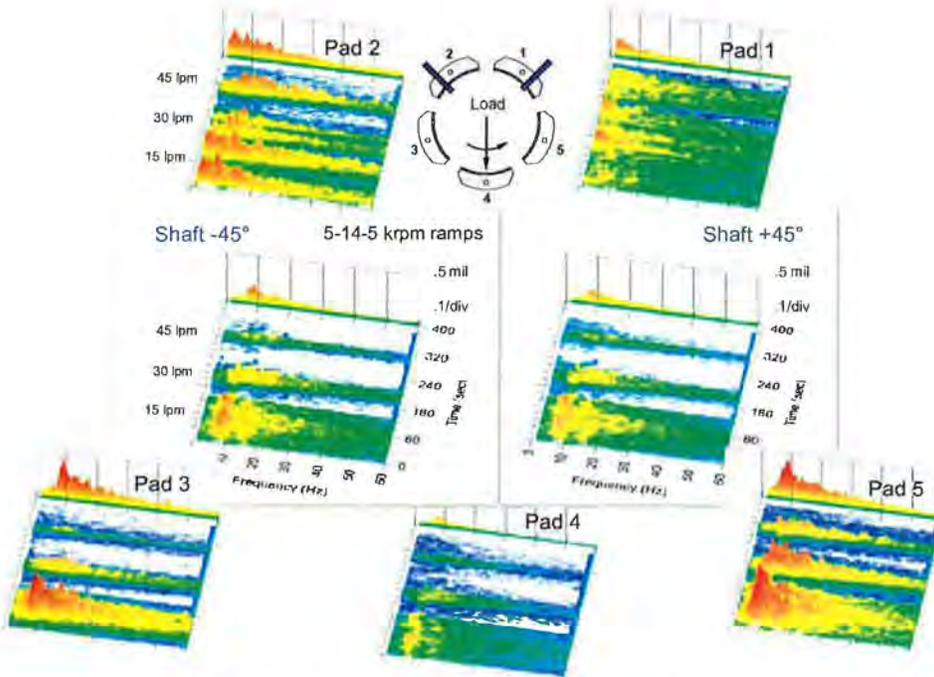
Figure 13. Direct lube LEG, LOP, 1.38 MPa, No SSV Grooves.

It can be noticed that the subsynchronous vibrations in unloaded pad 2 at 15 l/min do not correlate with either of the shaft probes (labeled -45° and +45°), which supports the apparent lack of correlation in previous tests. A unique observation is that the side pads 3 and 5, which were not monitored in previous tests, have the strongest subsynchronous vibrations and show excellent correlation with the shaft SSV hash indications.

7th EDF & LMS Poitiers Workshop: "Operational Limits of Bearings:
Improving of Performance through Modelling and Experimentation"

Futuroscope, October 2, 2008

The observations from Figure 13 relate to a specific bearing, orientation and load. Comparisons of test data for all five pads over a broad range of operating conditions for different bearing designs allowed for a generalized assessment of pad/shaft interaction.

The following observations and trends were found to be fairly common for all test bearings: All shaft SSV hash indications were confirmed to correlate with at least one of the five pads. Conversely, there were many instances where SSV from individual pads did not appear in shaft data. Shaft SSV hash most often correlated with the side pads. Figure 12 is helpful in the following explanations of this observation.

In the case of LBP under light load, side pad 1, 3, or both tended to correlate with shaft SSV hash. Pad 2 had more SSV hash than the side pads in many cases, but rarely correlated with the shaft indications. Noted earlier, shaft SSV hash decreased with load for LBP orientation, which is reasonable considering the high horizontal stiffness with the shaft supported between two bottom pads. At the same time, pads 1, 2 and 3 become less strongly coupled to the shaft as load increases and may still experience SSV hash, but with hydrodynamic forces too weak to affect the shaft.

For LOP under light load, the side pads (1, 2, 3, 5) individually or in combinations tended to correlate with shaft SSV hash. Correlation varied with bearing type and operating conditions, and is also likely influenced by any slight skew in the applied load vector and manufacturing height tolerance of individual pads for this particular orientation. Noted earlier, shaft SSV hash did not decrease as much with load for LOP orientation, which is reasonable considering the weak horizontal stiffness for this orientation. Pads 3 and 5 tended to correlate more with shaft SSV hash as load was applied. At the same time, pads 1 and 2 become less strongly coupled to the shaft and may still experience SSV hash, but with hydrodynamic forces too weak to affect the shaft.

3. Theoretical investigations

To help shed some light on these SSV hash measurements, the bearing geometry and operating conditions corresponding with data in Figure 13 were modeled using an algorithm developed by He [3]. This algorithm includes the effects of supply flowrate in its determination of a bearing's steady state (eccentricity, temperatures, power loss, etc.) and dynamic (stiffness and damping) performance based on the theories and experiments put forth by Heshmat [4]. Since the measurements presented in these SSV hash tests demonstrate the importance of supply flow on SSV, any theoretical investigation must account for supply flowrate effects.

3.1 Supply flowrate effects

The model applies to any bearing configuration where the supply flow is not sufficient to ensure a full film across all pads' surfaces. In this case, the model predicts a partial starvation at the inlet region of some of the pads. Unlike the full film situation where a continuous lubricant film starts at the pad leading edge, in a partially starved situation, the continuous film is formed downstream at some point where the clearance is sufficiently reduced. This physical phenomenon was observed and studied by Heshmat [4] on a two axial groove, sleeve bearing.
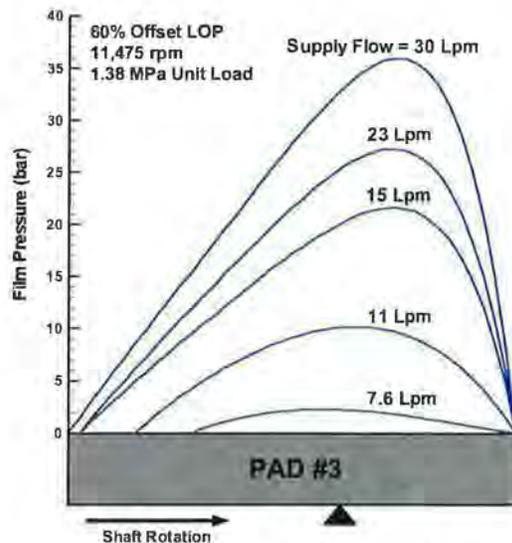
Figure 14. Partial starvation effects on pad film pressure.

Figure 14 illustrates predicted starvation effects for pad number 3, corresponding with test data pad numbers in Figure 13. With a supply flowrate of 30 l/min to the bearing, the film is able to generate pressure across the pad's entire arc length. Reducing flow to 15 l/min lowers the overall pressure distribution, but the pad still produces pressure across almost all of its arc length. The pad is partially starved at 11 l/min where no film pressure is produced at the inlet film region. Decreasing flow to 7.6 l/min expands the starved inlet region. At this flow, pressure levels are very small and the pivot is nearly centered within the positive pressure region. Partial starvation has effectively reduced the pad's pivot offset.

3.2 Pad Responsiveness

Since test results confirm that the individual pad motions are involved in this SSV hash phenomenon, the tilting pad bearing's full coefficients predicted by the modeling algorithm are of primary interest. For a tilting pad bearing with N_{pad} pads, the full coefficients consist of $5N_{pad}+4$ stiffness and $5N_{pad}+4$ damping coefficients. Described in detail in references [5] and [6], these full coefficients relate pad and shaft motions to forces and moments on the shaft and pads. For rotordynamic purposes, the magnitude of each individual coefficient is overlooked, focusing instead on their combined or "reduced" coefficients (four stiffnesses and four dampings). Closer scrutiny and understanding of these full coefficients is required when pad dynamics become the focus.

Table 1 presents stiffness full coefficients for a 60% offset, LOP, 5-pad bearing with 45 l/min supply flowrate where:

ΔF_x and ΔF_y = horizontal and vertical forces on the shaft.
Δx and Δy = horizontal and vertical shaft displacements.
$\Delta M_1 \dots \Delta M_5$ = moments on pads 1 through 5.
$\Delta \delta_1 \dots \Delta \delta_5$ = tilt angle changes on pads 1 through 5.

	Δx (mm)	Δy (mm)	$\Delta \delta_1$ (rad)	$\Delta \delta_2$ (rad)	$\Delta \delta_3$ (rad)	$\Delta \delta_4$ (rad)	$\Delta \delta_5$ (rad)
ΔF_x (E6 N)	0.587	0.155	1.543	-2.042	-6.285	2.277	7.17
ΔF_y (E6 N)	-0.227	0.807	2.74	2.219	-3.037	-14.50	-1.343
ΔM_1 (E6 N-mm)	-0.129	0.435	29.94	0	0	0	0
ΔM_2 (E6 N-mm)	-0.431	0.009	0	27.68	0	0	0
ΔM_3 (E6 N-mm)	-0.463	-1.148	0	0	75.92	0	0
ΔM_4 (E6 N-mm)	2.277	-2.086	0	0	0	182.3	0
ΔM_5 (E6 N-mm)	0.978	0.667	0	0	0	0	75.13

Table 1: Stiffness full coefficients for the 60% Offset LOP bearing, 11,475 rpm, 1.38 MPa

Each value in Table 1 represents a stiffness, either ΔF or ΔM divided by Δx, Δy, or $\Delta \delta$. Examining a few of the coefficients will help explain the physical meaning behind them. Tilt angle changes of the fourth pad ($\Delta \delta_4$) produce the largest vertical force on the shaft (ΔF_y), since it has the highest value of $K_{y\delta}$ (-14.5e6 N/rad). This is due to the fourth pad being on the bottom, supporting the majority of the load. Conversely, tilt angle changes on the second pad, located in the upper half of the bearing, produce a smaller vertical force on the shaft ($K_{y\delta}$ = 2.22e6 N/rad). The fourth pad is also the most difficult to tilt with the highest tilting stiffness $K_{\delta\delta}$ value (182.3e6 N-mm/rad), while the second pad is the easiest to tilt ($K_{\delta\delta}$ = 27.7e6 N-mm/rad). Tilting motions of the other four pads do not *directly* cause any moments on the loaded pad. The pads can only effectively communicate to each other through the shaft.

Some of the full coefficients along with the pads' polar inertia (I_p) form the equation of motion for pad tilting. A simplified version of this equation, using a pad's tilting stiffness $K_{\delta\delta}$ and damping $C_{\delta\delta}$, is given by:

$$I_p \ddot{\delta} + C_{\delta\delta} \dot{\delta} + K_{\delta\delta} \delta = M_{ext}$$

where M_{ext} is an external moment being applied. This equation can be used to examine the frequency response characteristics of each pad's tilting motion. Each pad's frequency response function (FRF) $H(\omega)$ is given by:

$$H(\omega) \equiv \frac{\delta(\omega)}{M_{ext}(\omega)} = \left\{ -\omega^2 I_p + j\omega C_{\delta\delta} + K_{\delta\delta} \right\}^{-1} \left[\frac{rad}{N-mm} \right]$$

An FRF's magnitude indicates how responsive a pad is to external moments trying to excite it. Examining the predicted FRFs of each pad as a function of supply flowrate provides for a direct comparison with the pad waterfall diagrams of the test data.

7th EDF & LMS Poitiers Workshop: "Operational Limits of Bearings: Improving of Performance through Modelling and Experimentation"

Futuroscope, October 2, 2008

Figure 15 presents the predicted H(ω) of pad 3 in Figure 13 as an example, focusing on the low frequency region below 60 Hz. Regardless of flow, the frequency response remains relatively flat as a function of excitation frequency with no peaks present. This is because the pad's tilting motions remain overdamped for all the flowrates examined. An overdamped system (critical damping greater than 100%) has no damped natural frequency, resulting in no peaks in its response.

It is unclear as to the exact cause of the 8 Hz peak in Figure 13's waterfall diagram for pad 3. One explanation is that there may be a predominant excitation at this frequency. Heshmat [4] observed a pulse excitation at similar low frequency levels in his starvation experiments on a sleeve bearing. Another possibility may be that the pad is actually underdamped which the model has not been able to predict. In this case, a broadband excitation would result in a definitive peak at the pad's damped natural frequency. Nothing indicates that the peak is associated with an unstable, self-excited phenomenon, since the pad's tilting damping $C_{\delta\delta}$ remains greater than or equal to zero. All indications are that the observed vibrations are forced in nature.

Both the measurements in Figure 13 and the predicted FRF in Figure 15 show that the third pad's overall responsiveness does dramatically increase as supply flow is reduced. According to the predictions in Figure 15, this pad responds very little to excitations until the bearing flow is reduced below approximately 15 l/min. This increased sensitivity correlates well with the predicted pressure profiles in Figure 14 and the test data in Figure 13. Below 15 l/min, the predictions in Figure 14 show that the pad becomes partially starved at the leading edge with low overall film pressures. These lower film pressures allow the pad to respond to external moment excitations more easily.
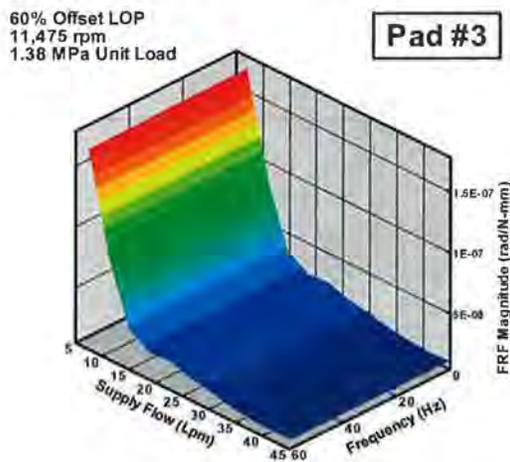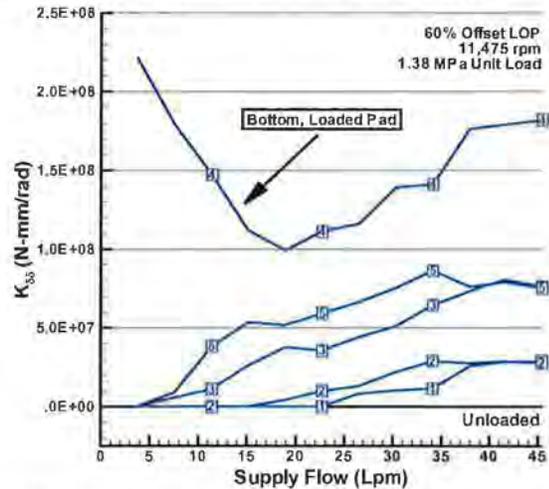

Figure 15. H(ω) with decreasing supply flow.

Figure 16. Tilting stiffness of individual pads versus supply flow.

According to the H(ω) equation, the low frequency responsiveness of an individual pad is largely dictated by its tilting stiffness, $K_{\delta\delta}$. Figure 16 presents the calculated tilting stiffness of all five pads as supply flow is varied. With the exception of the fourth pad, reducing supply flow causes a decrease in all the pads' tilting stiffnesses. Below 19 l/min, the fourth pad's stiffness begins to increase as it supports more of the entire bearing load. The strength of this tilting stiffness means the fourth pad does not easily respond to excitations, which correlates well with its relatively low vibrations in Figure 13.

When a pad becomes unloaded, it applies no pressure force on the shaft and its full coefficient stiffness and damping terms go to zero. The pad then moves like a rigid body and its tilting FRF is dictated by the polar inertia. The upper pads (1 and 2) become unloaded first as flow is reduced (Figure 16). This is because their larger film thicknesses require the most flow to maintain a full film along their entire surface. With smaller film thicknesses, the third and fifth pads remain loaded until below 7.5 l/min. These two pads' tilting stiffness values are low in magnitude at reduced flowrates, resulting in the increased responsiveness observed in Figure 15.

4. SSV groove design.

References from the early 90's [7, 8, 9, 10] document flow, power loss and pad temperature reductions of direct lube journal bearings attributed to the efficient evacuation of hot oil from the bearing cavity. The need to flood the direct lube bearing to eliminate SSV hash in initial investigations [1] correspondingly resulted in higher power loss, pad temperature, and oil flow requirements similar to a conventional, flooded bearing.

7th EDF & LMS Poitiers Workshop: "Operational Limits of Bearings: Improving of Performance through Modelling and Experimentation"

Futuroscope, October 2, 2008

The *SSV groove* modification [2] developed during 1999/2000 was pursued as a means to reduce SSV hash while maintaining some direct lube benefits, and has been successfully applied in many compressor, turbine, and gearbox applications. The design consists of narrow circumferential grooves, cut in the babbitt near the edges of the pads (Figure 17), to capture and redirect side leakage towards the leading edge of the next pad. In this way, additional oil is made available to the oil films without increasing the bulk flow to the bearing.

Figure 17. LEG® SSV grooves.

During initial development, the SSV groove design was based on hypotheses and shaft vibration data. To investigate the influence on pad vibration, SSV grooves were machined in the LEG pads used for data in Figure 13, and tested with the more advanced equipment currently available on the test rig. Results comparable to Figure 13 data are given in Figure 18.

The SSV groove tests confirmed that subsynchronous vibration levels in all pads were significantly reduced or eliminated over the full range of test operating conditions, for LOP and LBP orientations. Elimination of SSV hash at low bearing flow via additional oil from the grooves supports some of the theoretical assumptions regarding flow and pad responsiveness.
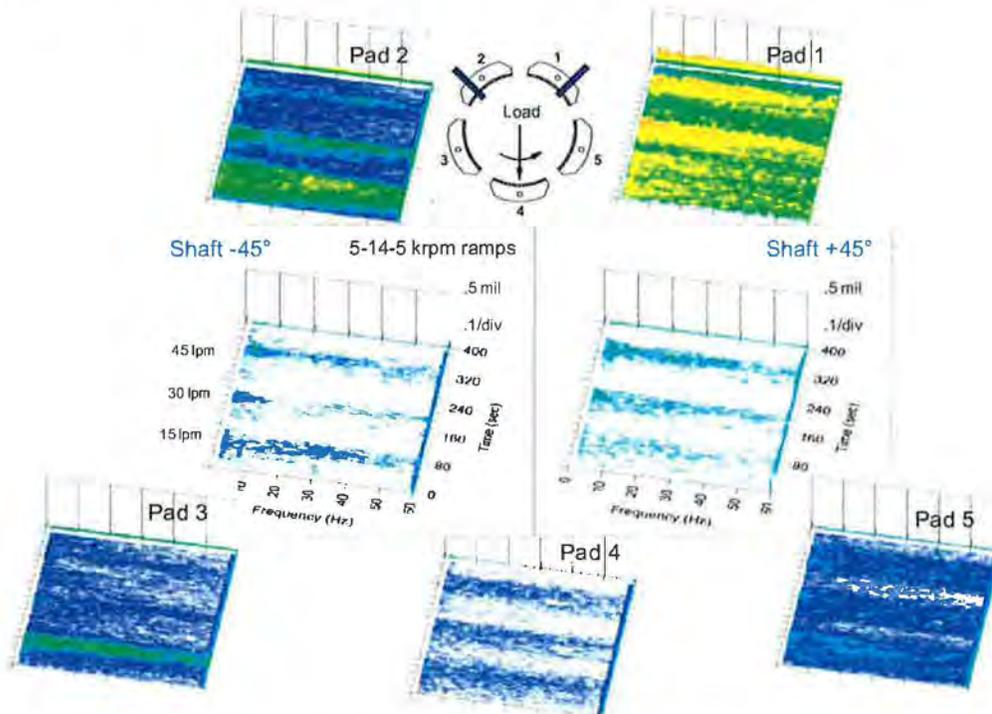

Figure 18. Direct lube LEG, LOP, 1.38 MPa, SSV Grooves.

7ʰ EDF & LMS Poitiers Workshop: "Operational Limits of Bearings:
Improving of Performance through Modelling and Experimentation"

Futuroscope, October 2, 2008

5. Discussions

The tests and analyses provide insight into the cause and nature of SSV hash, and information on parameters and methods successful in reducing or eliminating the signature. Field encounters over time have generated misinformation and concerns, which are discussed below in light of the test data and theoretical analyses presented.

5.1 Cause and nature

Test results indicate that shaft SSV hash is caused by pad vibrations. Babbitt damage from pad flutter is often mentioned as a concern, but is not the same phenomenon. Adams and Payandeh [11] studied pad flutter, which is attributed to self-excited, subsynchronous vibrations of unloaded pads with frequency ratios approximately 0.50 that of running speed. The damage is a result of violent, full clearance pad vibrations with forces sufficient to fatigue the babbitt.

The pad vibrations associated with SSV hash do not conform to these characteristics. SSV hash amplitudes are very small, more than an order of magnitude less than the bearing clearance, and frequency ratios are low, on the order of 0.10. Test results and analyses indicate that SSV hash has response characteristics indicative of a forced vibration. There were no means in the test rig to visualize flow in the films. However, Heshmat [4] did observe a periodic phenomenon in his visualization experiments of oil streamlets in an axial groove journal bearing, reported as a "pulse" that periodically transformed the starved region of the leading edge film into a pattern of oil streamlets. The pulse occurred every 0.5 to 1.0 seconds and its frequency varied with the degree of starvation. This phenomenon is consistent with the low frequencies and sensitivity at reduced flow encountered in SSV hash investigations.

5.2 Parameters and methods

Generalized field solutions based solely on flow to the oil films have often been unsuccessful. While test and analyses show oil flow is a contributing factor, they also show that flow is not the only key parameter. For example, SSV hash is encountered in conventional bearings where sufficient flow is available via a flooded cavity (e.g. Figure 9). The data suggests cavity pressure is another influential parameter. Calculated pressure drops in flooded designs indicate cavity pressures between 0.05 and 0.15 bar were present when SSV hash was noticeably reduced. On the other hand, there are cases where direct lube bearings operate at low flow with no SSV hash indications, the BPG at 15 l/min in Figure 11 for example. In this case, more flow actually produces higher SSV hash amplitudes.

Hindsight from test and analyses indicate proximity of individual pads to the shaft, their sensitivity to excitation, and the magnitude of their hydrodynamic forces are other key parameters. With multiple factors and complex pad/shaft interactions, evaluation needs to be performed by analysis rather than generalization. The analyses presented in the theory section are useful tools for assessing new designs and evaluating changes to existing designs.

6. Conclusions

This paper presents test results by Kingsbury, Inc., and theoretical analyses by BRG Machinery Consulting, LLC, performed to investigate a peculiar, low-frequency, low amplitude, broadband subsynchronous vibration, defined as *SSV hash*, that has been witnessed in different types of turbomachinery using tilting pad journal bearings. Based on a study of test results for conventional and direct lube designs over a broad range of operating conditions:

- There were more shaft SSV hash indications at low flow and low load. Amplitudes were sometimes higher at other operating conditions.
- Shaft SSV hash levels at light loads were similar for LBP and LOP orientation and decreased with applied load for LBP orientation, but there was only a small change with load for LOP orientation.
- Shaft SSV hash indications were confirmed to correlate with vibrations of at least one of the five pads. The side pads most often correlated with shaft SSV hash. The top upper pad for LBP orientation had the highest subsychronous indications in many cases, but rarely correlated with shaft data.
- Shaft SSV hash has been observed in conventional bearing designs at low oil flow. The data indicate that merely flooding the cavity is insufficient to suppress shaft SSV hash. At these conditions, direct lube designs operate with lower levels of shaft SSV hash, attributed to more direct application of oil to the film.
- At intermediate test oil flows, shaft SSV hash is more pronounced in evacuated, direct lube bearings and can be reduced, but not necessarily eliminated, by increasing oil flow. Amplitudes appear sensitive to certain operating conditions, around which are conditions where the evacuated direct lube bearings operated with negligible SSV hash indications.

7th EDF & LMS Poitiers Workshop: "Operational Limits of Bearings:
Improving of Performance through Modelling and Experimentation"

Futuroscope, October 2, 2008

The following conclusions are derived from the theoretical investigation of SSV hash:

- A tilting pad bearing's full coefficients can be used to assess the dynamics of individual pads.
- Using the full coefficients of one of the test bearings, theoretical investigations suggest that the observed SSV hash is likely a forced vibration phenomenon.
- Theoretical predictions indicate that a pad's responsiveness at low frequencies increases when there is insufficient oil to provide for a full film.
- At lower supply flowrates, predicted partial starvation at the leading edge progresses, which reduces the pad's tilting stiffness, making it more responsive to excitation.

There were two solutions determined from test data that eliminated the SSV hash signature:

- The first required flooding the bearing cavity, using labyrinth or floating seals and increased oil flow. The solution was effective for direct lube designs as well, but resulted in higher power loss, flow requirements, and pad temperatures comparable to a conventional, flooded design.
- The second was a modification consisting of patented SSV grooves cut in the babbitt near the edges of the pad, to capture and redirect side leakage towards the leading edge of the next pad. This was the only solution successful in eliminating SSV hash in an evacuated configuration. Low oil flow and power loss were maintained, with a slight penalty in pad temperature due to the introduction of warm, side leakage oil back into the oil film.

7. References

[1] DeCamillo S. (2006) Current issues regarding unusual conditions in high-speed turbomachinery. *Proceedings of the 5th EDF & LMS Poitiers Workshop*, Futuroscope. Keynote Presentation, pp. A.1-A.10.

[2] Wilkes J & DeCamillo S. (2002) Journal Bearing. *United States Patent No. 6,361,215 B1*, Mar. 26, 2002.

[3] He M. (2003) Thermoelastohydrodynamic analysis of fluid film journal bearings. *Ph.D. Dissertation, University of Virginia*, Charlottesville, Virginia.

[4] Heshmat H. (1991) The mechanism of cavitation in hydrodynamic lubrication. *STLE Tribology Transactions*, 34(2), 177-186.

[5] Shapiro W & Colsher R. (1977) Dynamic characteristics of fluid-film bearings. *Proceedings of the Sixth Turbomachinery Symposium*, Turbomachinery Laboratory, Texas A&M University, College Station, Texas, pp. 39-53.

[6] Parsell JK, Allaire PE & Barrett LE. (1983) Frequency effects in tilting-pad journal bearing dynamic coefficients. *ASLE Transactions*, 26(2), 222-227.

[7] Tanaka M. (1991) Thermohydrodynamic performance of a tilting pad journal bearing with spot lubrication. *ASME Journal of Tribology*, 113, 615-619.

[8] Harangozo AV, Stolarski TA & Gozdawa RJ. (1991) The effect of different lubrication methods on the performance of a tilting pad journal bearing. *STLE Tribology Transactions*, 34, 529-536.

[9] Brockwell K, Dmochowski W & DeCamillo S. (1992) Performance evaluation of the LEG tilting pad journal bearing. *IMechE Seminar Plain Bearings - Plain Bearings - Energy Efficiency and Design*, MEP, London, pp. 51-58.

[10] Fillon M, Bligoud JC & Frene J. (1993) Influence of the lubricant feeding method on the thermohydrodynamic characteristics of tilting pad journal bearings. *Proceedings of the 6th International Congress on Tribology*, Budapest, Hungary, Vol. 4, pp. 7-10.

[11] Adams ML & Payandeh S. (1983) Self-excited vibration of statically unloaded pads in tilting-pad journal bearings. *ASME Journal of Lubrication Technology*, 105, 377-384.

Acknowledgment